

Experimental charge density and topological properties of 3-(*tert*-butyloxycarbonylamino)bicyclo[1.1.1]pentanecarboxylic acid †

2 PERKIN

Peter Luger,^a Manuela Weber,^a Günter Szeimies^b and Michael Pätzelt^b

^a Institut für Chemie/Kristallographie, Freie Universität Berlin, Takustr. 6, 14195 Berlin, Germany

^b Institut für Organische und Bioorganische Chemie, Humboldt-Universität zu Berlin, Hessische Str. 1-2, 10115 Berlin, Germany. E-mail: luger@chemie.fu-berlin.de

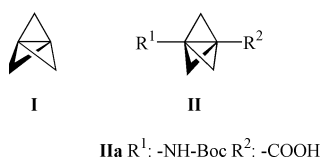
Received (in Cambridge, UK) 9th May 2001, Accepted 20th July 2001

First published as an Advance Article on the web 31st August 2001

The experimental charge density of a bicyclo[1.1.1]pentane cage derivative has been determined by X-ray diffraction at 110 K using conventional MoK α radiation and the CCD-area detection technique. A topological analysis using the AIM formalism yields quantitative bond topological descriptors on all covalent bonds, allowing an estimate of the corresponding bond strengths. The absence of a bond critical point between the bridgehead nuclei was confirmed; instead, a (3,+3) cage critical point \mathbf{r}_c was localized with $\rho(\mathbf{r}_c) = 0.68(2) \text{ e } \text{Å}^{-3}$, in close agreement with earlier theoretical calculations.

Introduction

In the oligocyclic cages of [1.1.1]propellane (**I**) and related bicyclo[1.1.1]pentane derivatives (**II**) distances between the bridgehead atoms of 1.58–1.60 Å for type **I** derivatives and 1.80–1.91 Å for compounds of type **II** are reported,¹ raising the question of the covalent or noncovalent nature of the interbridge linkage.² Theoretical calculations and application of the AIM formalism (AIM = atoms in molecules)³ gave an indication that a bridgehead bond is present in the propellanes but not in the bicyclo[1.1.1]pentane cage. This was concluded from the clear identification of a bond critical point only for **I**, whereas a cage critical point was found in **II**. Experimental charge density studies of appropriate **I** and **II** derivatives should contribute to the bonding/nonbonding question. Unfortunately the parent, unsubstituted [1.1.1]propellane, is not suitable for an experimental charge density study⁴ due to severe disorder problems in the crystal structure.



Previous qualitative electron difference density studies gave neither for type **I**⁵ nor for type **II** derivatives^{6,7} any indication of bond density maxima between the bridgehead atoms. However, in no case was a topological analysis performed in the experimental studies.^{5–7} Hence a comparison with the quantitative findings from the AIM calculation of Wiberg *et al.*³ was not possible. Here we present an experimental charge density study on 3-(*tert*-butyloxycarbonylamino)bicyclo[1.1.1]pentanecarboxylic acid (**IIa**) based on high resolution X-ray diffraction data collected at 110 K which allowed the derivation of quantitative topological descriptors from the experimental electron density.

† Electronic supplementary information (ESI) available: multipole population coefficients and a summary of topological descriptors from experiment and theoretical calculations. See <http://www.rsc.org/suppdata/p2/b1/b104062f/>

Experimental

The title compound is a protected derivative of the novel 3-aminobicyclo[1.1.1]pentanecarboxylic acid. This compound can be considered as a rigid analogue of 4-aminobutyric acid, which acts as a neurotransmitter in the brain. Crystals suitable for X-ray analysis were prepared by slow evaporation from diethyl ether.⁸ A colorless crystal with the dimensions $0.6 \times 0.4 \times 0.3 \text{ mm}^3$ was chosen for the experiment. Accurate X-ray data were measured on a BRUKER SMART 1000 diffractometer using MoK α -radiation. The temperature was maintained at 110 K during the measurement with an N₂-gas stream cooling device. Data were collected for two different positions of the CCD area detector. For the 2θ positions -32° and -72° a total number of 4431 frames were collected with a scan width of 0.3° in ω and an exposure time of 30 and 120 s, respectively. The measurement strategy was planned with the ASTRO program,⁹ the data collection was monitored with the SMART program⁹ and the frames were integrated with the SAINT⁹ program. 29337 reflections were measured up to a resolution of $\sin \theta/\lambda = 1.09 \text{ Å}^{-1}$ (or $d = 0.46 \text{ Å}$). Further details on the crystal data and the experimental conditions are given in Table 1.

Starting atomic parameters from an earlier crystal structure analysis⁸ were used as input for an aspherical atom refinement with the program package XD,¹⁰ that makes use of the Hansen–Coppens multipole formalism.¹¹ The charge density is modelled by a superposition of pseudoatoms represented by a nucleus-centered multipole expansion [eqn. (1)].

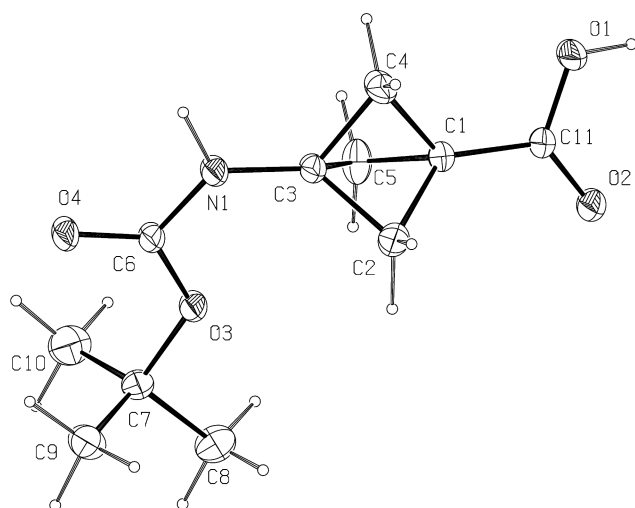
$$\rho_{\text{atom}}(\mathbf{r}) = \rho_{\text{core}}(\mathbf{r}) + P_v \kappa^3 \rho_v(\kappa \mathbf{r}) + \sum_{l=0}^{l_{\text{max}}} \kappa'^3 R_l(\kappa' r) \sum_{m=0}^l P_{lm\pm} Y_{lm\pm}(\theta, \phi, r) \quad (1)$$

The first two terms represent the spherical core (ρ_{core}) and valence density (ρ_v) composed of Hartree–Fock wave functions expanded over Slater-type basis functions for the heavy atoms. The scattering factors of the hydrogen atoms were calculated from the exact radial density functions using a fixed expansion–contraction parameter $\kappa = 1.20$. This contraction allows a simple analytical approximation to the scattering factor introduced by Stewart *et al.*¹² The deformation of the valence density is represented by real spherical harmonic angular functions $Y_{lm\pm}$ and normalized Slater-type radial functions R_l with energy-optimized exponents.¹³ In the least-squares refinement

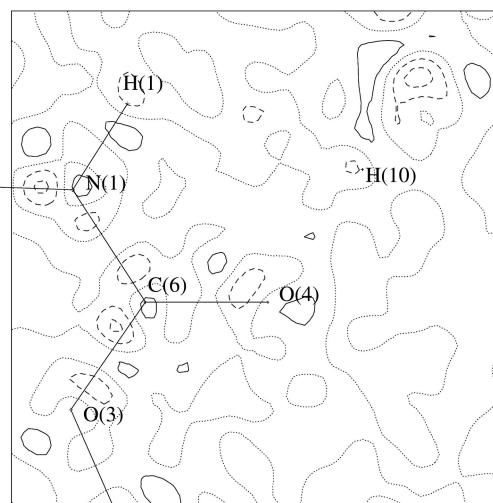
Table 1 Crystal data and structure refinement for 3-(*tert*-butyloxycarbonylamino)bicyclo[1.1.1]pentanecarboxylic acid^a

Empirical formula	C ₁₁ H ₁₇ NO ₄
Formula weight/g mol ⁻¹	146.15
Crystal system	Monoclinic
Space group	<i>Cc</i>
<i>Z</i>	4
Temperature/K	110
Unit cell dimensions:	
<i>a</i> /Å	6.0581(1)
<i>b</i> /Å	18.1774(5)
<i>c</i> /Å	11.2293(3)
β /°	92.94(1)
<i>V</i> /Å ³	1234.95(5)
Calculated density/g cm ⁻³	1.222
<i>F</i> (000)	488
Absorption coefficient μ /mm ⁻¹	0.09
Crystal size/mm ³	0.6 × 0.4 × 0.3
λ /Å	0.7107
($\sin \theta/\lambda$) _{max} /Å ⁻¹	1.09
Limiting indices	-12 ≤ <i>h</i> ≤ 13, -38 ≤ <i>k</i> ≤ 39, -23 ≤ <i>l</i> ≤ 24
Number of collected reflections	29337
Symmetry independent reflections	6786
Reflections with <i>F</i> _o > 3σ(<i>F</i> _o)	6090
Completeness	98%
Redundancy	4.3
<i>R</i> _{int}	0.019
<i>N</i> _{ref} / <i>N</i> _{var} ^b	15.2
<i>R</i> _w (multipole)	0.018
<i>R</i> ₁ (multipole)	0.022
<i>R</i> _{all} (<i>F</i>) (multipole)	0.027
Gof	3.39

^a CCDC reference number 163809. See <http://www.rsc.org/suppdata/p2/b1/b104062f/> for crystallographic files in .cif or other electronic format. ^b *N*_{ref}/*N*_{var} is the ratio between the number of reflections and the number of variables.

**Fig. 1** ORTEP²² representation of the molecular structure of **IIa**, indicating the atomic numbering scheme used. Displacement ellipsoids are drawn at a 50% probability level.

the expansion–contraction parameters κ and the populations P_v and $P_{lm\pm}$ were refined along with the positional and thermal parameters of each atom. The hexadecapolar level of the multipolar expansion was used for carbon, nitrogen and oxygen while dipoles were used for the hydrogen atoms. In order to account for chemical symmetry and to reduce the number of variables, local site symmetries and constraints were imposed. A local mirror symmetry was applied to the atoms N(1), O(3) and C(6), mm2 symmetry to the methylene carbon atoms and 3m symmetry to the atoms of the *tert*-butyl group, respectively (atomic numbering scheme, see Fig. 1). No symmetry restrictions were imposed on the carboxy group and the O(4) of the amide group because the atoms were involved in several hydrogen bonds. The densities of the methylene carbons C(2), C(4) and C(5) and the methyl carbons C(8), C(9), C(10) were constrained to be the same. This was also applied to the hydrogen

**Fig. 2** Residual map in the plane of the amide group. Positive, negative and zero contours are represented by solid, dashed and dotted lines, respectively. Contour intervals at 0.05 e Å⁻³.

atoms of the latter groups. The hydrogens were moved to the distances determined by neutron diffraction.¹⁴ The molecule was kept neutral during the refinement (neutrality constraint). In the multipole model used, a scale factor, the atomic positions, anisotropic and isotropic temperature parameters of the heavy and of the hydrogen atoms, were refined together with the multipole parameters. The refinement of the 6090 unique reflections ($F_{\text{obs}}(\mathbf{H}) > 3\sigma(F_{\text{obs}}(\mathbf{H}))$) yielded agreement factors of $R = 2.2\%$ and $R_w = 1.8\%$. Experimental residual maps do not show any significant residues of the electron density; no contours greater than 0.1 e Å⁻³ could be found after the multipole refinement, indicating an adequate fit of the multipole model to the experimental data. Fig. 2 shows exemplarily the practically featureless residual density map in the plane of the amide group.

Table 2 Summary of experimental topological data at critical points: d is the internuclear distance, Δb_p is the difference between this quantity and the bond path length, ρ and $\nabla^2\rho$ were calculated at the experimental critical points

Atoms	$d/\text{\AA}$	$\Delta b_p/\text{\AA}$	$\rho/e \text{\AA}^{-3}$	$\nabla^2\rho/e \text{\AA}^{-5}$	Type
C(1)–C(4)	1.5548(7)	0.0023	1.53(3)	–9.69(9)	(3,–1)
C(1)–C(2)	1.5612(7)	0.0051	1.60(2)	–10.66(8)	(3,–1)
C(1)–C(5)	1.5553(6)	0.0071	1.59(3)	–11.39(8)	(3,–1)
C(3)–C(4)	1.5493(7)	0.0048	1.63(3)	–12.63(9)	(3,–1)
C(3)–C(2)	1.5613(6)	0.0059	1.65(2)	–13.07(7)	(3,–1)
C(3)–C(5)	1.5554(7)	0.0052	1.67(3)	–13.07(7)	(3,–1)
C(1)–C(11)	1.4949(6)	0.0002	1.94(3)	–21.4(10)	(3,–1)
C(7)–C(8)	1.5215(7)	0.0000	1.89(2)	–20.02(6)	(3,–1)
C(7)–C(9)	1.5220(7)	0.0018	1.86(2)	–18.87(7)	(3,–1)
C(7)–C(10)	1.5242(8)	0.0016	1.86(2)	–18.85(7)	(3,–1)
C(3)–N(1)	1.4331(6)	0.0003	1.99(4)	–27.3(2)	(3,–1)
C(6)–N(1)	1.3579(6)	0.0001	2.52(4)	–26.7(2)	(3,–1)
C(7)–O(3)	1.4845(7)	0.0000	1.81(4)	–19.4(2)	(3,–1)
C(11)–O(1)	1.3257(8)	0.0004	2.49(4)	–32.5(3)	(3,–1)
C(6)–O(3)	1.3294(6)	0.0002	2.60(4)	–33.4(2)	(3,–1)
C(11)–O(2)	1.2274(7)	0.0001	3.09(5)	–36.1(4)	(3,–1)
C(6)–O(4)	1.2406(7)	0.0005	3.11(5)	–42.0(3)	(3,–1)
C(1)⋯C(3)	1.8680(6)	—	0.68(2)	11.09(6)	(3,+3)
Averages:					
C–C _{cage}	1.556(4)	0.0050	1.61(5)	–11.8(13)	(3,–1)
C(sp ³)–C(sp ³)	1.523(1)	0.0011	1.87(2)	–19.2(50)	(3,–1)

Theoretical calculations

The GAUSSIAN98 program package¹⁵ was used for several *ab initio* calculations which were executed at the Hartree–Fock (HF) and the density functional (B3LYP) level of theory. In all cases the 6-311+G(d,p) basis set was used. A geometry optimization was executed at the HF level, followed by a B3LYP single point calculation. In addition, single-point calculations at HF and B3LYP levels were performed at the experimental geometry. The wave functions obtained were evaluated with the program package AIMPAC.¹⁶

Results and discussion

In a previous study the structure of **IIa** was determined from a spherical refinement of room temperature data and the molecular geometry was discussed.⁸ The molecule consists of a large, almost planar fragment where the only (non-H) out-of-plane atoms are the cage atoms C(2)/C(5) and the methyl C atoms C(9)/(10).

Two intermolecular hydrogen bonds with the carboxy O(1)–H and the amino N(1)–H as donors connect molecules *via* the crystallographic glide plane [N(1)–H⋯O(2) (H⋯O = 2.077, N⋯O = 3.090(1) Å, N–H⋯O = 164°, symmetry: $-1 + x, 1 - y, -1/2 + z$) and O(1)–H⋯O(4) (H⋯O = 1.654, O(1)⋯O(4) = 2.593(1) Å, O–H⋯O = 168°, symmetry: $1 + x, 1 - y, 1/2 + z$].

Compared to the spherical room temperature structure all bond lengths after multipole refinement (see Table 2) are, by 0.01 Å, longer. The interbridge distance C(1)⋯C(3) of 1.8680(6) Å is not far from the value of 1.87 Å reported from an electron-diffraction study.¹⁷ The agreement between experimental (multipole) geometry and that from an optimization at the HF/6-311+G(d,p) level is within 0.02 Å for most bond lengths with the major exception of the C–O bonds C(11)–O(2) and C(6)–O(4) (about 0.05 Å). These are sites where intermolecular hydrogen bonds exist, which are not considered in the *ab initio* optimization of the isolated molecule.

Static deformation densities are defined as the difference between the atom centered multipole density and the charge density of a hypothetical spherical promolecule ($\Delta\rho_{\text{def}}(\mathbf{r}) = \sum_{\text{all atoms}}[\rho_{\text{mult}}(\mathbf{r}) - \rho_{\text{pro}}(\mathbf{r})]$). In Fig. 3 static deformation density maps are shown in that section of the bicyclo[1.1.1]pentane cage which is part of the main molecular plane (Fig. 3a) and in a plane containing the strong O(1)–H⋯O(4) hydrogen bond (Fig. 3b). On all covalent bonds and in the oxygen lone pair

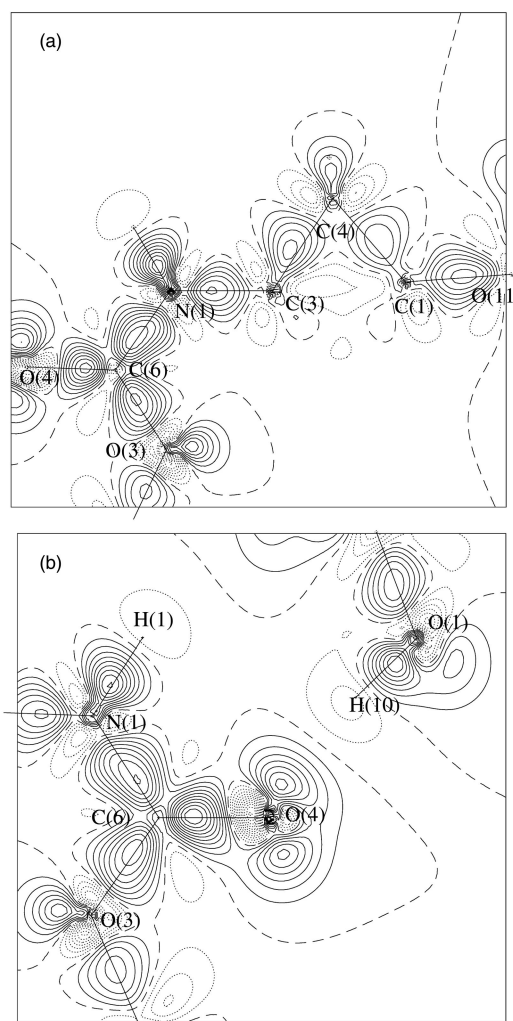


Fig. 3 Static deformation density map (a) in one of the cage planes (C(3)–C(4)–C(1)) and (b) in the plane of the amide group, containing also the strong O(1)–H⋯O(4) hydrogen bond. Contour intervals at 0.1 e Å⁻³; for further explanation see Fig. 2.

regions properly resolved density maxima are visible. Due to the cage strain the maxima on C(3)–C(4) and C(1)–C(4) are shifted outward from the direct vectors between these atoms,

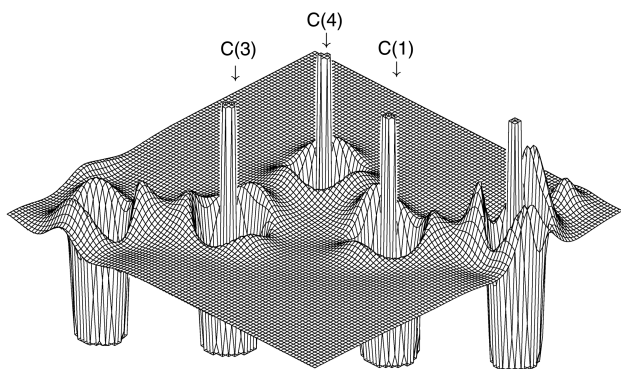


Fig. 4 Relief representation of the negative Laplacian in the cage plane C(3)–C(4)–C(1).

illustrating the bent character of these bonds. The same features are seen in the C(2) and C(5) containing wings of the cage. There is no density between the bridgehead atoms C(1) and C(3). While the lack of charge between the bridgehead nuclei in the electron density difference map has to be interpreted with care and was even considered as “an artifact of the promolecule distributions”,³ properties directly deducible from the total charge density, such as the Laplacian $\nabla^2\rho(\mathbf{r})$ are more reliable. The topology of the negative Laplacian in the plane C(3)–C(4)–C(1) is displayed in Fig. 4. While the typical saddle shaped regions significant for covalent bonds are clearly visible on C(3)–C(4) and C(1)–C(4), this is not seen between C(1) and C(3). The static map in the hydrogen bond region (Fig. 3b) shows an asymmetric deformation of the O(4) lone pair under the influence of the strong hydrogen bond, expressed by the short O...O contact of 2.593(1) Å.

To get a quantitative description of the electronic structure of **IIa** a full topological analysis¹⁸ was performed with the XDPROP part of the XD program package.¹⁰ On all covalent bonds (3, –1) bond critical points (bcp's, defined by the property that at a bcp \mathbf{r}_b the gradient of ρ vanishes, *i.e.* $\nabla\rho(\mathbf{r}_b) = 0$) were identified. No bcp was found between C(1) and C(3), but a (3, +3) critical cage point was found inside the cage.

Table 2 gives a summary of quantitative experimental topological properties at the critical points. A quantitative com-

parison between all experimental and theoretical properties is deposited in the Supplementary Information. There are three types of C–C bonds in the structure: the single bonds in the *tert*-butyl group, the cage C–C bonds and the bond C(1)–C(11) to the carboxylic group. Their different strengths are clearly indicated by the $\rho(\mathbf{r}_b)$ values. Compared to the average of 1.87(2) e Å^{–3} for the single bonds, C(1)–C(11) is stronger (1.94(3) e Å^{–3}) while the cage C–C bonds are significantly weaker. The experimental bond length after multipole refinement averaged over the six cage C–C bonds is 1.556(4) Å, compared to the theoretical value of 1.546 Å from HF/6-311+G(d,p) (this work) and HF/6-31G* (Wiberg *et al.*³). The bent character of the cage bonds is indicated by the differences Δb_p between the direct internuclear separations and the bond path lengths (Table 2). These differences, mean 0.005 Å, are nevertheless rather small, but were also found in this range in the cyclopropane ring of the bullvalene cage.¹⁹ Rather pronounced are the differences in $\rho(\mathbf{r}_b)$ and its Laplacian for the two different carbon–nitrogen bonds. C(6)–N(1) as part of the amide group possesses partial double bond character. The five C–O bonds are listed in Table 2 in increasing $\rho(\mathbf{r}_b)$ order. C(7)–O(3) is the weakest, the formal double bonds C(11)–O(2) and C(6)–O(4) are the strongest ones.

To compare experimental and theoretical bond topological data Fig. 5 shows a plot of $\rho(\mathbf{r}_b)$ values *versus* corresponding bond lengths. They should be related by an exponential function but can roughly be fitted by a straight line in the considered bond length range. If the corresponding linear fits of the Hartree–Fock (HF) and B3LYP density functional (DF) results are compared with the experimental distribution, it can be seen that for the C–C bonds (bond lengths > 1.5 Å) the agreement is rather close, while the gap becomes wider with decreasing length (< 1.45 Å), the range where most of the C–N and C–O bonds are found. This is even more pronounced for the Laplacians (not shown, see Table in deposition material). This problem with polar bonds was recognized in earlier studies;²⁰ Volkov *et al.*²¹ reported that the reason is an insufficient flexibility of the radial functions in the multipole model.

The (3, +3) cage critical point inside the bicyclo[1.1.1]pentane fragment is located at almost equal distances of 0.93 Å from the bridgehead atoms and at somewhat longer distances (1.23–1.27 Å) from the other cage defining carbon atoms. Its topological

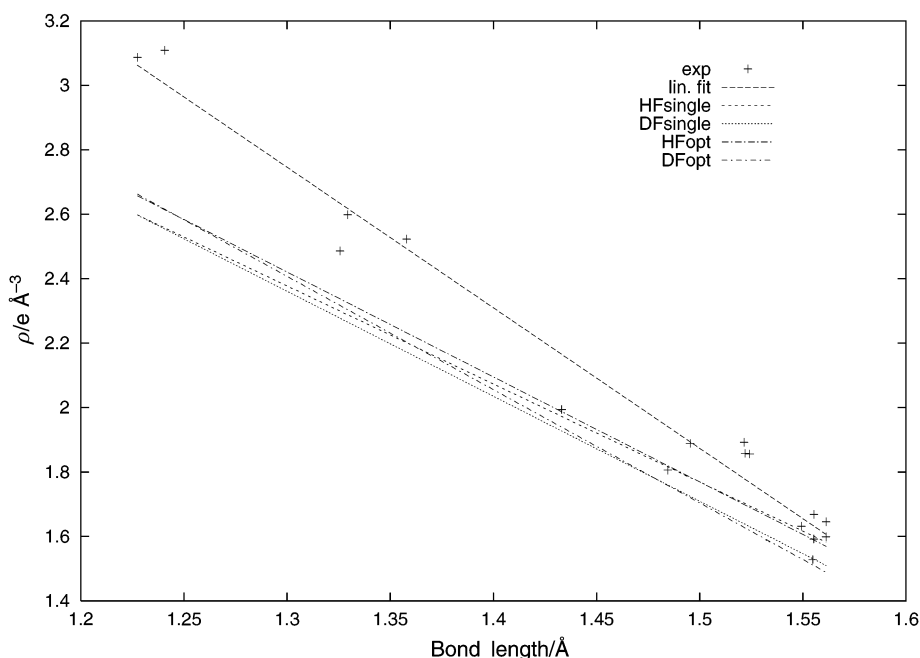


Fig. 5 $\rho(\mathbf{r}_b)$ values plotted *versus* corresponding bond lengths. Dots indicate the experimental values, fitted by a linear function (lin. fit). The other straight lines refer to theoretical data: Hartree–Fock (HFsingle) and B3LYP (DFsingle) single-point calculations at the experimental geometry, and HF and B3LYP calculations at the HF/6-311+G(d,p) optimized geometry, respectively (HFopt, DFopt).

descriptors, $\rho(\mathbf{r}_c) = 0.68(2) \text{ e } \text{\AA}^{-3}$, $\nabla^2\rho(\mathbf{r}_c) = 11.09(6) \text{ e } \text{\AA}^{-5}$ are in almost perfect agreement with previous and present theoretical findings. Wiberg *et al.*³ reported $\rho(\mathbf{r}_c) = 0.66 \text{ e } \text{\AA}^{-3}$ from HF/6-31G*; our calculations gave $\rho(\mathbf{r}_c) = 0.67/0.69 \text{ e } \text{\AA}^{-3}$, $\nabla^2\rho(\mathbf{r}_c) = 12.03/11.26 \text{ e } \text{\AA}^{-5}$ on HF/B3LYP levels.

Conclusion

The present study has verified the recent progress in experimental charge density work. In less than one week a high resolution X-ray data set was measured with almost standard laboratory equipment in that conventional MoK α -radiation and a conventional area detection technique were used which in short will replace the serial counter technique completely. The obtained accuracy, documented by crystallographic agreement factors of around 2%, indicates that charge density data collection can be considered now as a fast, precise and routine X-ray diffraction experiment.

Secondly, the method no longer provides qualitative results only, but also reliable quantitative topological descriptors. Especially, the magnitudes of $\rho(\mathbf{r})$ at the bond critical points \mathbf{r}_b give an estimate of the nature and the strength of a chemical bond. The topology of the Laplace function and the presence/absence of a bond critical point in a region between two atoms are a reliable indication of the existence/nonexistence of a covalent bond.

For the topology of the bicyclo[1.1.1]pentane cage the theoretical predictions of Wiberg *et al.*³ were completely confirmed by experiment, even quantitatively. It would be of particular interest now to execute an analogous experimental charge density study of an appropriate [1.1.1]propellane derivative.

Acknowledgements

We thank the Bundesminister für Forschung und Technologie (BMBF), Grant No. 05SM8KEA0, and the Fonds der Chemischen Industrie for financial support.

References

- 1 M. D. Levin, P. Kaszynski and J. Michl, *Chem. Rev.*, 2000, **100**, 169.
- 2 J. E. Jackson and L. C. Allen, *J. Am. Chem. Soc.*, 1984, **106**, 591.
- 3 K. B. Wiberg, R. F. W. Bader and C. D. H. Lau, *J. Am. Chem. Soc.*, 1987, **109**, 985.

- 4 P. Seiler, *Helv. Chim. Acta*, 1990, **73**, 1574.
- 5 P. Chakrabarti, P. Seiler, J. D. Dunitz, A.-D. Schlüter and G. Szeimies, *J. Am. Chem. Soc.*, 1981, **103**, 7378.
- 6 P. Seiler, J. Belzner, U. Bunz and G. Szeimies, *Helv. Chim. Acta*, 1988, **71**, 2100.
- 7 H. Irngartinger, W. Reimann, P. Dowd and P. Garner, *J. Chem. Soc., Chem. Commun.*, 1990, 429.
- 8 P. Luger, M. Weber, G. Szeimies and M. Pätzler, *Acta Crystallogr., Sect. C*, 2000, **56**, 1170.
- 9 Programs ASTRO (1995–1996), SMART (1996), SAINT (1994–1996), Bruker-AXS Inc., Madison, Wisconsin, USA.
- 10 T. Koritsanszky, S. Howard, P. R. Mallinson, Z. Su, T. Richter and N. K. Hansen, XD-a Computer Program Package for Multipole Refinement and Analysis of Electron Densities from Diffraction Data. *User manual*, Freie Universität Berlin, 1995.
- 11 N. K. Hansen and P. Coppens, *Acta Crystallogr., Sect. A*, 1978, **34**, 909.
- 12 R. F. Stewart and E. R. Davidson, *J. Chem. Phys.*, 1965, **42**, 3175.
- 13 E. Clementi and C. Roetti, *Atomic Data and Nuclear Data Tables*, 1974, **14**, 177.
- 14 T. F. Koetzle, M. N. Frey, M. S. Lehmann and W. C. Hamilton, *Acta Crystallogr., Sect. B*, 1973, **29**, 2571.
- 15 M. J. Frisch, G. W. Trucks, H. B. Schlegel, G. E. Scuseria, M. A. Robb, J. R. Cheeseman, V. G. Zakrzewski, J. A. Montgomery, Jr., R. E. Statmann, J. C. Burant, S. Dapprich, J. M. Millam, A. D. Daniels, K. N. Kudin, M. C. Strain, O. Farkas, J. Tomasi, V. Barone, M. Cossi, R. Cammi, B. Mennucci, C. Pomelli, C. Adamo, S. Clifford, J. Ochterski, G. A. Petersson, P. Y. Ayala, Q. Cui, K. Morokuma, D. K. Malick, A. D. Rabuck, K. Raghavachari, J. B. Foresman, J. Cioslowski, J. V. Ortiz, B. B. Stefanov, G. Liu, A. Liashenko, P. Piskorz, I. Komaromi, R. Gomperts, R. L. Martin, D. J. Fox, T. Keith, M. A. Al-Laham, C. Y. Peng, A. Nanayakkara, C. Gonzalez, M. Challacombe, P. M. W. Gill, B. Johnson, W. Chen, M. W. Wong, J. L. Andres, C. Gonzalez, M. Head-Gordon, E. S. Replogle and J. A. Pople, Gaussian, Inc., Pittsburgh, PA, 1998.
- 16 J. Cheeseman, T. A. Keith and R. F. W. Bader, AIMPACK program package, McMaster University, Hamilton, Ontario, 1992.
- 17 A. Almenningen, B. Andersen and B. A. Nyhus, *Acta Chem. Scand.*, 1971, **25**, 1217.
- 18 R. F. W. Bader, *Atoms in Molecules: A Quantum Theory*, Number 22 in The International Series of Monographs on Chemistry, Clarendon Press, Oxford, 2nd edn., 1995.
- 19 T. Koritsanszky, J. Buschmann and P. Luger, *J. Phys. Chem.*, 1996, **100**, 10541.
- 20 W. D. Arnold, L. K. Sanders, M. T. McMahon, A. V. Volkov, G. Wu, P. Coppens, S. R. Wilson, N. Godbout and E. Oldfield, *J. Am. Chem. Soc.*, 2000, **122**, 4708.
- 21 A. Volkov, Y. Abramov, P. Coppens and C. Gatti, *Acta Crystallogr., Sect. A*, 2000, **56**, 332.
- 22 M. N. Burnett and C. K. Johnson, ORTEP-III, Oak Ridge Thermal Ellipsoid Plotting Program for Crystal Structure Illustrations ORNL-6895, Oak Ridge National Laboratory, 1996.